

We are IntechOpen, the world's leading publisher of Open Access books Built by scientists, for scientists

6,900

Open access books available

185,000

International authors and editors

200M

Downloads

Our authors are among the

154

Countries delivered to

TOP 1%

most cited scientists

12.2%

Contributors from top 500 universities



WEB OF SCIENCE™

Selection of our books indexed in the Book Citation Index
in Web of Science™ Core Collection (BKCI)

Interested in publishing with us?
Contact book.department@intechopen.com

Numbers displayed above are based on latest data collected.
For more information visit www.intechopen.com



Calorimetric Determination of Heat Capacity, Entropy and Enthalpy of Mixed Oxides in the System CaO–SrO–Bi₂O₃–Nb₂O₅–Ta₂O₅

Jindřich Leitner, David Sedmidubský, Květoslav Růžička and Pavel Svoboda

Additional information is available at the end of the chapter

<http://dx.doi.org/10.5772/54064>

1. Introduction

Mixed oxides in the system CaO–SrO–Bi₂O₃–Nb₂O₅–Ta₂O₅ possess many extraordinary electric, magnetic and optical properties for which they are used in fabrication of various electronic components. For example Sr₂(Nb,Ta)₂O₇ and (Sr,Ca)Bi₂(Nb,Ta)₂O₉ are used for ferroelectric memory devices, CaNb₂O₆, Sr₅(Nb_{1-x}Ta_x)₄O₁₅ and Bi(Nb,Ta)O₄ for microwave dielectric resonators and Ca₂Nb₂O₇ as non-linear optical materials and hosts for rare-earth ions in solid-state lasers. Ternary strontium bismuth oxides SrBi₂O₄, Sr₂Bi₂O₅, and Sr₆Bi₂O₉ are of considerable interest due to a visible light driven photocatalytic activity.

To assess the thermodynamic stability and reactivity of these oxides under various conditions during their preparation, processing and operation, a complete set of consistent thermodynamic data, including heat capacity, entropy and enthalpy of formation, is necessary. Some of these data are available in literature. Akishige et al. [1] have been measured the heat capacities of Sr₂Nb₂O₇ and Sr₂Ta₂O₇ single crystals in the temperature range 2-600 K. The results have been only plotted and the values of $S^{\circ}_m(298)$ have not been calculated. A commensurate transformation of Sr₂Nb₂O₇ at $T_{INC} = 495$ K has been observed accompanied by changes in enthalpy and entropy of $\Delta H = 291$ J mol⁻¹ and $\Delta S = 0.587$ J K⁻¹ mol⁻¹. The heat capacity of Sr₂Nb₂O₇ has been also measured by Shabbir et al. [2] in the temperature range 375-575 K. They have observed a phase transition at $T_{INC} = 487 \pm 2$ K connected with $\Delta H = 147 \pm 14$ J mol⁻¹ and $\Delta S = 0.71 \pm 0.10$ J K⁻¹ mol⁻¹. The heat capacities of polycrystalline and monocrystalline SrBi₂Ta₂O₉ and Sr_{0,85}Bi_{2,1}Ta₂O₉ have been measured by Onodera et al. [3–5] at 80-800 K. Morimoto et al. [6] have reported the results of the heat capacity measurements of SrBi₂(Nb_xTa_{1-x})₂O₉ ($x = 0, 1/3, 2/3$ a 1). The temperature dependences of heat capacities show lambda-transitions with maxima at the Currie temperature $T_c = 570 \pm 1$ K, 585 ± 2 K, 625 ± 3 K a 690 ± 2 K for $x = 0, 1/3, 2/3$ and 1 ,

respectively. Using EMF (electromotive force) measurements, Raghavan has obtained the values of the Gibbs energy of formation from binary oxides, $\Delta_{ox}G$, for some niobates [7,8] and tantalates [9,10] of calcium. His results are summarized in Table 1. The same technique has been employed by Dneprova et al. [11] for $\Delta_{ox}G$ measurement for CaNb_2O_6 and $\text{Ca}_2\text{Nb}_2\text{O}_7$. Their results presented in Table 1 are not significantly different from the results of Raghavan. Using the CALPHAD approach [13], Yang et al. [14] have assessed thermodynamic data for various mixed oxides in the $\text{SrO-Nb}_2\text{O}_5$ system. The same approach has been used by Hallstedt et al. for the assessment of thermodynamic data of mixed oxides in the systems $\text{CaO-Bi}_2\text{O}_3$ [14] and $\text{SrO-Bi}_2\text{O}_3$ [15]. Besides equilibrium data, values of the enthalpy of formation [16] of mixed oxide have been considered. Later on, these systems have been studied by EMF method by Jacob and Jayadevan [17,18] and temperature dependences of $\Delta_{ox}G$ for various mixed oxides have been derived. These data have been included into the thermodynamic re-assessment of the $\text{CaO-SrO-Bi}_2\text{O}_3$ system [19].

Oxide	$\Delta_{ox}G$ (kJ mol ⁻¹)	T (K)	$\Delta_{ox}H$ (kJ mol ⁻¹)	$\Delta_{ox}S$ (J K ⁻¹ mol ⁻¹)	Ref.
CaNb_2O_6	$-75.82 - 0.03345T$	1245-1300	-75.82	33.45	[7]
$\text{Ca}_2\text{Nb}_2\text{O}_7$	-178.44	1256			[8]
$\text{Ca}_3\text{Nb}_2\text{O}_8$	-209.94	1256			[8]
$\text{CaTa}_4\text{O}_{11}$	$-36.982 - 0.029T$	1250-1300	-36.98	29.0	[9]
CaTa_2O_6	-65.14	1250			[10]
$\text{Ca}_2\text{Ta}_2\text{O}_7$	-102.82	1250			[10]
$\text{Ca}_4\text{Ta}_2\text{O}_9$	-165.05	1250			[10]
CaNb_2O_6	$-175.73 + 0.02259T$	1100-1276	-175.73	-22.59	[11]
$\text{Ca}_2\text{Nb}_2\text{O}_7$	$-212.54 - 0.02218T$	1100-1350	-212.54	22.18	[11]
$\text{Sr}_2\text{Nb}_{10}\text{O}_{27}$	$-1125.69 + 0.35069T$	298-5000	-1125.69	-350.69	[12]
SrNb_2O_6	$-325.04 + 0.05865T$	298-5000	-325.04	-58.65	[12]
$\text{Sr}_2\text{Nb}_2\text{O}_7$	$-367.43 + 0.03993T$	298-5000	-367.43	-39.93	[12]
$\text{Sr}_5\text{Nb}_4\text{O}_{14}$	$-746.72 + 0.05101T$	298-5000	-746.72	-51.01	[12]
$\text{Ca}_5\text{Bi}_{14}\text{O}_{26}$	$-125.90 - 0.055T$	298-1300	-125.9	55.0	[19]
CaBi_2O_4	$-27.60 - 0.003T$	298-1300	-27.6	3.0	[19]
$\text{Ca}_4\text{Bi}_6\text{O}_{13}$	$-97.60 - 0.008T$	298-1300	-97.6	8.0	[19]
$\text{Ca}_2\text{Bi}_2\text{O}_5$	$-42.20 - 0.003T$	298-1300	-42.2	3.0	[19]
SrBi_2O_4	$-63.86 - 0.0018T$	298-1300	-63.86	1.8	[19]
$\text{Sr}_2\text{Bi}_2\text{O}_5$	$-118.75 + 0.024T$	298-1300	-118.75	-24.0	[19]
$\text{Sr}_3\text{Bi}_2\text{O}_6$	$-109.60 + 0.0024T$	298-1300	-109.60	-2.4	[19]

Table 1. Published values of $\Delta_{ox}G$, $\Delta_{ox}H$ a $\Delta_{ox}S$ for some mixed oxides in the system $\text{CaO-SrO-Bi}_2\text{O}_3\text{-Nb}_2\text{O}_5\text{-Ta}_2\text{O}_5$

This review brings a summary of our results [20–30] focused on calorimetric determination of heat capacity, entropy and enthalpy of mixed oxides in the system CaO–SrO–Bi₂O₃–Nb₂O₅–Ta₂O₅. Temperature dependences of molar heat capacity in a broad temperature range were evaluated from the experimental heat capacity and relative enthalpy data. Molar entropies at $T = 298.15$ K were calculated from low temperature heat capacity measurements. Furthermore, the results of calorimetric measurements of the enthalpies of drop-solution in a sodium oxide-molybdenum oxide melt for several stoichiometric mixed oxides in the above mentioned system are reported from which the values of enthalpy of formation from constituent binary oxides were derived. Finally, some empirical estimation and correlation methods (the Neumann-Kopp's rule, entropy-volume correlation and electronegativity-differences method) for evaluation of thermodynamic data of mixed oxides are tested and assessed.

2. Experimental

Nineteen mixed oxides in the system CaO–SrO–Bi₂O₃–Nb₂O₅–Ta₂O₅ with stoichiometry CaBi₂O₄, Ca₄Bi₆O₁₃, Ca₂Bi₂O₅, SrBi₂O₄, Sr₂Bi₂O₅, CaNb₂O₆, Ca₂Nb₂O₇, SrNb₂O₆, Sr₂Nb₂O₇, Sr₂Nb₁₀O₂₇, Sr₅Nb₄O₁₅, BiNbO₄, BiNb₅O₁₄, BiTaO₄, Bi₄Ta₂O₁₁, Bi₇Ta₃O₁₈, Bi₃TaO₇, SrBi₂Nb₂O₉, and SrBi₂Ta₂O₉ were prepared, characterized and examined. The samples were prepared by conventional solid state reactions from high purity precursors (CaCO₃, SrCO₃, Bi₂O₃, Nb₂O₅ and Ta₂O₅). A three step procedure was used consisting of an initial calcination run of mixed powder precursors and subsequent double firing of prereacted mixtures pressed into pellets. The phase composition of the prepared samples was checked by X-ray powder diffraction (XRD). XRD data were collected at room temperature with an X'Pert PRO (PANalytical, the Netherlands) θ - θ powder diffractometer with parafocusing Bragg-Brentano geometry using CuK α radiation ($\lambda = 1.5418$ nm). Data were scanned over the angular range 5–60° (2θ) with an increment of 0.02° (2θ) and a counting time of 0.3 s step⁻¹. Data evaluation was performed by means of the HighScore Plus software.

The PPMS equipment 14 T-type (Quantum Design, USA) was used for the heat capacity measurements in the low temperature region [31–35]. The measurements were performed by the relaxation method [36] with fully automatic procedure under high vacuum (pressure $\sim 10^{-2}$ Pa) to avoid heat loss through the exchange gas. The samples were compressed powder pellets. The densities of the samples were about 65 % of the theoretical ones.

The samples were mounted to the calorimeter platform with cryogenic grease Apiezon N (supplied by Quantum Design). The procedure was as follows: First, a blank sample holder with the Apiezon only was measured in the temperature range approx. 2–280 K to obtain background data, then the sample plate was attached to the calorimeter platform and the measurement was repeated in the same temperature range with the same temperature steps. The sample heat capacity was then obtained as a difference between the two data sets. This procedure was applied, because the heat capacity of Apiezon is not negligible in comparison with the sample heat capacity (~ 8 % at room temperature) and exhibits a peak-shaped transition below room temperature [37]. The manufacturer claims the precision of this

measurement better than 2 % [38]; the control measurement of the copper sample (99.999 % purity) confirmed this precision in the temperature range 50–250 K. However, the precision of the measurement strongly depends on the thermal coupling between the sample and the calorimeter platform. Due to unavoidable porosity of the sample plate this coupling is rapidly getting worse as the temperature raises above 270 K and Apiezon diffuses into the porous sample. Consequently, the uncertainty of the obtained data tends to be larger.

A Micro DSC III calorimeter (Setaram, France) was used for the heat capacity determination in the temperature range of 253–352 K. First, the samples were preheated in a continuous mode from room temperature up to 352 K (heating rate 0.5 K min^{-1}). Then the heat capacity was measured in the incremental temperature scanning mode consisting of a number of 5–10 K steps (heating rate 0.2 K min^{-1}) followed by isothermal delays of 9000 s. Two subsequent step-by-step heating were recorded for each sample. Synthetic sapphire, NIST Standard reference material No. 720, was used as the reference. The uncertainty of heat capacity measurements is estimated to be better than $\pm 1 \%$.

Enthalpy increment determinations were carried out by drop method using high-temperature calorimeter, Multi HTC 96 (Setaram, France). All measurements were performed in air by alternating dropping of the reference material (small pieces of synthetic sapphire, NIST Standard reference material No. 720) and of the sample (pressed pellets 5 mm in diameter) being initially held at room temperature, through a lock into the working cell of the preheated calorimeter. Endothermic effects are detected and the relevant peak area is proportional to the heat content of the dropped specimen. The delays between two subsequent drops were 25–30 min. To check the accuracy of measurement, the enthalpy increments of platinum in the temperature range 770–1370 K were measured first and compared with published reference values [39]. The standard deviation of 22 runs was 0.47 kJ mol^{-1} , the average relative error was 2.0 %. Estimated overall accuracy of the drop measurements is $\pm 3 \%$.

The heats of drop-solution were determined using a Multi HTC 96 high-temperature calorimeter (Setaram, France). A sodium oxide-molybdenum oxide melt of the stoichiometry $3\text{Na}_2\text{O} + 4\text{MoO}_3$ was used as the solvent. The ratio of solute/solvent varied from 1/250 up to 1/500. The measurements were performed at temperatures of 973 and 1073 K in argon or air atmosphere. The method consists in alternating dropping of the reference material (small spherules of pure platinum) and of the sample (small pieces of pressed tablets 10–40 mg), being initially held near room temperature (T_0), through a lock into the working cell (a platinum crucible with the solvent) of the preheated calorimeter at temperature T . Two or three samples were examined during one experimental run. The delays between two subsequent drops were 30–60 min. The total heat effect ($\Delta_{\text{ds}}H$) includes the heat of solution ($\Delta_{\text{sol}}H$), the heat content of the sample ($\Delta_{\text{T}}H$), and, for the carbonates, the heat of decomposition ($\Delta_{\text{decomp}}H$) to form solid CaO or SrO and gaseous CO_2 . Using appropriate thermochemical cycles, the values of the enthalpy of formation of mixed oxides from the binary oxides and from the elements at 298 K were evaluated. The temperature dependence of the heat capacity of platinum [39] was used for the calculation of the sensitivity of the calorimeters.

2.1. Characterization of prepared samples

The XRD analysis revealed that the prepared samples were without any observable diffraction lines from unreacted precursors or other phases. The lattice parameters of the oxides were evaluated by Rietveld refinement [40] and are summarized in Table 2 together with the values of theoretical density calculated from the lattice parameters.

2.2. Evaluation of temperature dependence of heat capacity at low temperatures

The fit of the low-temperature heat capacity data (LT fit) consists of two steps. Assuming the validity of the phenomenological formula $C_{pm} = \beta T^3 + \gamma_{el}T$, at $T \rightarrow 0$ where β is proportional to the inverse cube root of the Debye temperature Θ_D and $\gamma_{el}T$ is the Sommerfeld term, we plotted the C_{pm}/T vs. T^2 dependence for $T < 8$ K to estimate the Θ_D and γ_{el} values. Since all compounds under study are semiconductors with a sufficiently large band gap, the non-zero γ_{el} values are supposed to be either due to some metallic impurities or to a series of Schottky-like transitions resulting from structure defects. Nevertheless, they are negligible in most cases (typically < 0.5 mJ K⁻² mol⁻¹) and can be ignored in further analysis. As an example, the results of heat capacity measurements on CaNb₂O₆ and LT fit for $T < 10$ K is shown in Fig. 1.

Oxide	<i>a</i> (nm)	<i>b</i> (nm)	<i>c</i> (nm)	α (°)	β (°)	γ (°)	<i>d</i> (g cm ⁻³)	Ref.
CaBi ₂ O ₄	1.66143	1.15781	1.39915	90	134.03	90	6.631	[20]
Ca ₄ Bi ₆ O ₁₃	0.59308	1.73512	0.72192	90	90	90	6.540	[20]
Ca ₂ Bi ₂ O ₅	1.01074	1.01249	1.04618	116.88	107.16	92.98	6.468	[20]
SrBi ₂ O ₄	1.92635	0.43437	0.61444	90	95.50	90	7.392	[29]
Sr ₂ Bi ₂ O ₅	1.42935	0.61715	0.76478	90	90	90	6.628	[29]
CaNb ₂ O ₆	1.49698	0.57472	0.52202	90	90	90	4.760	[26]
Ca ₂ Nb ₂ O ₇	0.76853	1.33587	0.54959	90	90	98.29	4.496	[26]
SrNb ₂ O ₆	0.77209	0.55930	1.09821	90	90.37	90	5.174	[24]
Sr ₂ Nb ₂ O ₇	0.39544	2.67735	0.57004	90	90	90	5.206	[26]
Sr ₂ Nb ₁₀ O ₂₇	3.715	3.697	0.3943	90	90	90	5.653	a)
Sr ₅ Nb ₄ O ₁₅	0.56576	0.56576	1.14536	90	90	120	5.490	[27]
BiNbO ₄	0.56893	1.1728	0.49915	90	90	90	7.297	[21]
BiNb ₅ O ₁₄	1.76762	1.72072	0.39610	90	90	90	4.948	b)
BiTaO ₄	0.56394	1.1776	0.49626	90	90	90	9.149	[21]
Bi ₄ Ta ₂ O ₁₁	0.66159	0.76528	0.98781	101.39	90.10	89.99	9.306	[28]
Bi ₇ Ta ₃ O ₁₈	3.40162	0.76054	0.66354	90	109.16	90	9.395	[28]
Bi ₃ TaO ₇	0.54711	0.54711	0.54711	90	90	90	9.327	[28]
SrBi ₂ Nb ₂ O ₉	0.55160	0.55087	2.51020	90	90	90	7.275	[22]
SrBi ₂ Ta ₂ O ₉	0.55224	0.55266	2.50124	90	90	90	8.801	[22]

a) Quoted according to JCPDS 035-1220.

b) Quoted according to JCPDS 048-0986

Table 2. Structural characterization of prepared samples

In the second step of the LT fit, both sets of the C_{pm} data (relaxation time + DSC) were considered. Analysis of the phonon heat capacity was performed as an additive combination of Debye and Einstein models. Both models include corrections for anharmonicity, which is responsible for a small, but not negligible, additive term at higher temperatures and which accounts for the difference between isobaric and isochoric heat capacity. According to literature [41], the term $1/(1 - \alpha T)$ is considered as a correction factor.

The acoustic part of the phonon heat capacity is described using the Debye model

$$C_{phD} = \frac{9R}{1 - \alpha_D T} \left(\frac{T}{\Theta_D} \right)^3 \int_0^{x_D} \frac{x^4 \exp(x)}{[\exp(x) - 1]^2} dx \quad (1)$$

where R is the gas constant, Θ_D is the Debye characteristic temperature, α_D is the coefficient of anharmonicity of acoustic branches and $x_D = \Theta_D/T$. Here the three acoustic branches are taken as one triply degenerate branch. Similarly, the individual optical branches are described by the Einstein model

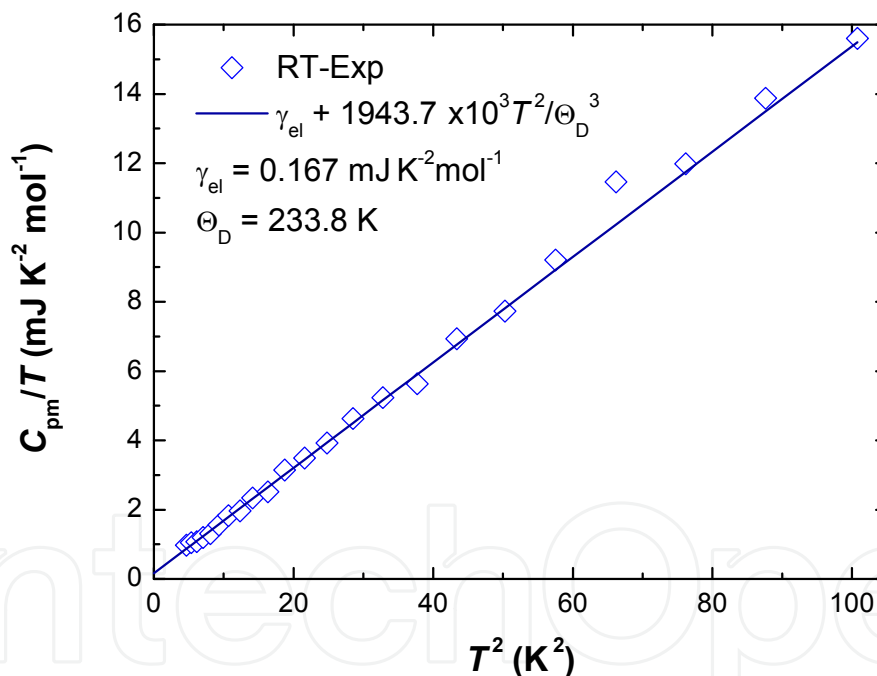


Figure 1. Temperature dependence of C_{pm}/T function for CaNb_2O_7 at low temperatures

$$C_{phEi} = \frac{R}{1 - \alpha_{Ei} T} \frac{x_{Ei}^2 \exp(x_{Ei})}{[\exp(x_{Ei}) - 1]^2} \quad (2)$$

where α_{Ei} and $x_{Ei} = \Theta_{Ei}/T$ have analogous meanings as in the previous case. Several optical branches are again grouped into one degenerate multiple branch with the same Einstein characteristic temperature and anharmonicity coefficient. The phonon heat capacity then reads

$$C_{\text{ph}} = C_{\text{phD}} + \sum_{i=1}^{3n-3} C_{\text{phE}i} \quad (3)$$

All the estimated values were further treated by a simplex routine and a full non-linear fit was performed on all adjustable parameters.

The values of relative enthalpies at 298.15 K, $H_m(298.15) - H_m(0)$, were evaluated from the low-temperature C_{pm} data (LT fit) by numerical integration of the $C_{pm}(T)$ dependences from zero to 298.15 K. Standard deviations (2σ) were calculated using the error propagation law. The values of standard molar entropies at 298.15 K, $S_m(298.15)$, were derived from the low-temperature C_{pm} data (LT fit) by numerical integration of the $C_{pm}(T)/T$ dependences from zero to 298.15 K. A numerical integration was used with the boundary conditions $S_m = 0$ and $C_{pm} = 0$ at $T = 0$ K. Standard deviations (2σ) were calculated using the error propagation law. All calculated values are summarized in Table 3.

Oxide	$C_{pm}(298)$ (J K ⁻¹ mol ⁻¹)	$H_m(298)-H_m(0)$ (J mol ⁻¹)	$S_m(298)$ (J K ⁻¹ mol ⁻¹)	$\Delta_{\text{ox}}S$ (J K ⁻¹ mol ⁻¹)	Ref.
CaBi ₂ O ₄	151.3	26470 ± 158	188.5 ± 3.3	1.9	[20]
Ca ₄ Bi ₆ O ₁₃	504.1	85079 ± 507	574.1 ± 8.8	-23.8	[20]
Ca ₂ Bi ₂ O ₅	197.4	33735 ± 201	231.3 ± 2.9	6.6	[20]
SrBi ₂ O ₄	155.6	29601 ± 169	206.1 ± 1.1	4.0	[29]
Sr ₂ Bi ₂ O ₅	201.9	38199 ± 219	261.2 ± 1.4	5.5	[29]
CaNb ₂ O ₆	171.8	28159 ± 170	167.3 ± 0.9	-8.1	[26]
Ca ₂ Nb ₂ O ₇	218.1	35631 ± 215	212.4 ± 1.2	-1.1	[26]
SrNb ₂ O ₆	170.2	28722 ± 174	173.9 ± 0.9	-17.0	[24]
Sr ₂ Nb ₂ O ₇	216.6	37977 ± 266	238.5 ± 1.3	-5.9	[26]
Sr ₂ Nb ₁₀ O ₂₇	746.8	124150 ± 740	759.7 ± 4.1	-33.9	[27]
Sr ₅ Nb ₄ O ₁₅	477.2	83340 ± 490	524.5 ± 2.8	-18.4	[27]
BiNbO ₄	121.3	22120 ± 134	147.9 ± 0.8	5.0	[21]
BiNb ₅ O ₁₄	386.8	62639 ± 362	397.2 ± 2.1	-25.8	[23]
BiTaO ₄	119.3	22021 ± 132	149.1 ± 0.8	3.3	[21]
Bi ₄ Ta ₂ O ₁₁	363.2	66566 ± 384	449.6 ± 2.3	9.5	[28]
Bi ₇ Ta ₃ O ₁₈	602.7	109760 ± 634	743.0 ± 3.8	8.6	[28]
Bi ₃ TaO ₇	235.2	44265 ± 254	304.3 ± 1.6	10.0	[28]
SrBi ₂ Nb ₂ O ₉	286.4	49230 ± 292	327.2 ± 1.7	-12.2	[22]
SrBi ₂ Ta ₂ O ₉	286.6	49060 ± 289	339.2 ± 1.8	-5.9	[22]

Table 3. Heat capacity, relative enthalpy, entropy and entropy of formation from binary oxides at temperature 298.15 K of various mixed oxides in the system CaO–SrO–Bi₂O₃–Nb₂O₅–Ta₂O₅

A comparison is given in Table 4 of the values of entropy of formation from binary oxides $\Delta_{\text{ox}}S$ at 298 K calculated from our results and those from literature. The values of $\Delta_{\text{ox}}S$ are calculated using the relation

$$\Delta_{\text{ox}}S = S_{\text{m}}(\text{MO}) - \sum_i b_i S_{\text{m}}(\text{BO},i) \quad (4)$$

where $S_{\text{m}}(\text{MO})$ and $S_{\text{m}}(\text{BO},i)$ stand for the molar entropies of a mixed oxide and a binary oxide i , respectively, and b_i is a constitution coefficient representing the number of formula units of a binary oxide i per formula unit of the mixed oxide. The following values were used for calculation: $S_{\text{m}}(\text{CaO}, 298.15 \text{ K}) = 38.1 \text{ J K}^{-1} \text{ mol}^{-1}$ [42], $S_{\text{m}}(\text{SrO}, 298.15 \text{ K}) = 53.58 \text{ J K}^{-1} \text{ mol}^{-1}$ [43], $S_{\text{m}}(\text{Bi}_2\text{O}_3, 298.15 \text{ K}) = 148.5 \text{ J K}^{-1} \text{ mol}^{-1}$ [44], $S_{\text{m}}(\text{Nb}_2\text{O}_5, 298.15) = 137.30 \text{ J K}^{-1} \text{ mol}^{-1}$ [45] $S_{\text{m}}(\text{Ta}_2\text{O}_5, 298.15) = 143.09 \text{ J K}^{-1} \text{ mol}^{-1}$ [45]. Furthermore, $S_{\text{m}}(\text{Sr}_2\text{Nb}_2\text{O}_7, 298.15) = 238.5 \text{ J K}^{-1} \text{ mol}^{-1}$ from this work can be directly compared with the value $232.37 \text{ J K}^{-1} \text{ mol}^{-1}$ obtained by numeric integration of the $C_{\text{pm}}(T)/T$ dependences from zero to 298.15 K given in Ref. [1]. It should be noted that the values of entropy assessed by thermodynamic optimization of phase equilibrium data are generally considered as less reliable as the values derived from low temperature heat capacity measurements. It is due to possible strong correlation between the enthalpy and entropy contributions to the Gibbs energy. So the obvious discrepancies between our values and data from assessments [12,19] could be explain in this way.

Oxide	$\Delta_{\text{ox}}S^{\text{a)}$ ($\text{J K}^{-1} \text{ mol}^{-1}$)	$\Delta_{\text{ox}}S$ ($\text{J K}^{-1} \text{ mol}^{-1}$)	Ref.
CaNb ₂ O ₆	-8.1	33.45	[7]
		-22.59	[11]
Ca ₂ Nb ₂ O ₇	-1.1	22.18	[11]
Sr ₂ Nb ₁₀ O ₂₇	-34.0	-350.69	[12]
SrNb ₂ O ₆	-17.0	-58.65	[12]
Sr ₂ Nb ₂ O ₇	-6.0	-39.93	[12]
Sr ₅ Nb ₄ O ₁₄	-18.0	-51.01	[12]
CaBi ₂ O ₄	1.9	3.0	[19]
Ca ₄ Bi ₆ O ₁₃	-23.8	8.0	[19]
Ca ₂ Bi ₂ O ₅	6.6	3.0	[19]
SrBi ₂ O ₄	4.0	1.8	[19]
Sr ₂ Bi ₂ O ₅	5.5	-24.0	[19]

^{a)} This work

Table 4. The values of entropy of formation from binary oxides at 298.15 K: a comparison of our results and data from literature

It should be noted that the thorough analysis of the Debye and Einstein contributions to the heat capacities reveals that the different vibrational modes contribute to the total values of $\Delta_{\text{ox}}S$ to a different extent and partial compensation is possible in some cases.

2.3. Evaluation of heat capacity at temperatures above 298 K

For the assessment of temperature dependences of C_{pm} above room temperature, the heat capacity data from DSC and the enthalpy increment data from drop calorimetry were treated simultaneously by the linear least-squares method (HT fit). The temperature dependence of C_{pm} was considered in the form

$$C_{pm} = A + BT + C/T^2 \quad (5)$$

thus the related temperature dependence of $\Delta H_m(T) = H_m(T) - H_m(T_0)$ is given by equation

$$\Delta H_m(T) = H_m(T) - H_m(T_0) = \int_{T_0}^T C_{pm} dT = A(T - T_0) + B(T^2 - T_0^2)/2 - C(1/T - 1/T_0) \quad (6)$$

The sum of squares which is minimized has the following form

$$F = \sum_{i=1}^{N(C_p)} w_i^2 [C_{pm,i} - A - BT_i - C/T_i^2]^2 + \sum_{j=1}^{N(\Delta H)} w_j^2 [\Delta H_{m,j} - A(T_j - T_{0,j}) - B(T_j^2 - T_{0,j}^2)/2 + C(1/T_j - 1/T_{0,j})]^2 \rightarrow \min \quad (7)$$

where the first sum runs over the C_{pm} experimental points while the second sum runs over the ΔH_m experimental points. Different weights w_i (w_j) were assigned to individual points calculated as $w_i = 1/\delta_i$ ($w_j = 1/\delta_j$) where δ_i (δ_j) is the absolute deviation of the measurement estimated from overall accuracies of measurements (1 % for DSC and 3 % for drop calorimetry). Both types of experimental data thus gain comparable significance during the regression analysis. To smoothly connect the LT fit and HT fit data the values of $C_{pm}(298.15)$ from LT fit were used as constraints and so Eq. (7) is modified

$$F_{constr} = F - \lambda [C_{pm}(298.15) - A - 298.15B - C/298.15^2] \rightarrow \min \quad (8)$$

The numerical values of parameters A , B and C are now obtained by solving a set of equations deduced as derivatives of F_{constr} with respect of these parameters and a multiplier λ which are equal to zero at the minimum of F_{constr} . Assessed values of parameters A , B and C of Eq. (4) for mixed oxides are presented in Table 5.

As an example, the results of heat capacity measurements and relative enthalpy measurements on Bi₇Ta₃O₁₈ [28] are shown in Fig. 2. Empirical estimation according to the Neumann-Kopp's rule (NKR) is also plotted for comparison.

The empirical Neumann-Kopp's rule (NKR) is frequently used for estimation of unknown values of the heat capacity of mixed oxides [46–48]. According to NKR, heat capacity of a mixed oxide is calculated as a sum of heat capacities of the constituent binary ones

$$C_{pm}(\text{MO}) = \sum_i b_i C_{pm}(\text{BO}, i) \quad (9)$$

It was concluded [47,48] that NKR predicts the heat capacities of mixed oxides remarkably well around room temperature but the deviations (mostly positive) from NKR become substantial at higher temperatures. Mean relative error of the estimated values of $C_{pm}(298.15\text{ K})$ is 1.4 %. Calculated temperature dependences of $\Delta_{ox}C_{pm} = C_{pm}(\text{MO}) - \sum b_i C_{pm}(\text{BO}, i)$ for various mixed oxides in the systems CaO–Nb₂O₅, SrO–Nb₂O₅ and Bi₂O₃–Ta₂O₅ are shown in Fig. 3.

Oxide	$C_{pm} = A + B \cdot T + C/T^2$ (J K ⁻¹ mol ⁻¹)			Temperature range (K)	Ref.
	A	10 ³ B	10 ⁻⁶ C		
CaBi ₂ O ₄	157.161	38.750	-1.546	298-1000	[20]
Ca ₄ Bi ₆ O ₁₃	550.808	114.890	-7.201	298-1200	[20]
Ca ₂ Bi ₂ O ₅	226.096	33.374	-3.432	298-1100	[20]
SrBi ₂ O ₄	161.97	45.936	-1.7832	298-1100	[29]
Sr ₂ Bi ₂ O ₅	197.48	87.463	-1.9282	298-1200	[29]
CaNb ₂ O ₆	200.40	34.32	-3.45	298-1500	[26]
Ca ₂ Nb ₂ O ₇	257.20	36.21	-4.435	298-1400	[26]
SrNb ₂ O ₆	200.47	29.37	-3.473	298-1500	[24]
Sr ₂ Nb ₂ O ₇	248.00	43.50	-3.948	298-1400	[26]
Sr ₂ Nb ₁₀ O ₂₇	835.351	227.648	-13.904	298-1400	[27]
Sr ₅ Nb ₄ O ₁₅	504.796	147.981	-6.376	298-1400	[27]
BiNb ₄ O ₄ ^{a)}	128.628	33.400	-1.991	150-1200	[21]
BiNb ₅ O ₁₄	455.840	60.160	-7.734	298-1400	[23]
BiTa ₄ O ₄ ^{b)}	133.594	25.390	-2.734	150-1200	[21]
Bi ₄ Ta ₂ O ₁₁	445.8	5.451	-7.489	298-1400	[28]
Bi ₇ Ta ₃ O ₁₈	699.0	52.762	-9.956	298-1400	[28]
Bi ₃ TaO ₇	251.6	67.05	-3.237	298-1400	[28]
SrBi ₂ Nb ₂ O ₉	324.470	63.710	-5.076	298-1400	[22]
SrBi ₂ Ta ₂ O ₉	320.220	64.510	-4.700	298-1400	[22]

^{a)} An extra term $1.363 \times 10^8/T^3$ was added.

^{b)} An extra term $2.360 \times 10^8/T^3$ was added.

Table 5. Parameters of temperature dependence of molar heat capacities of various mixed oxides in the system CaO–SrO–Bi₂O₃–Nb₂O₅–Ta₂O₅

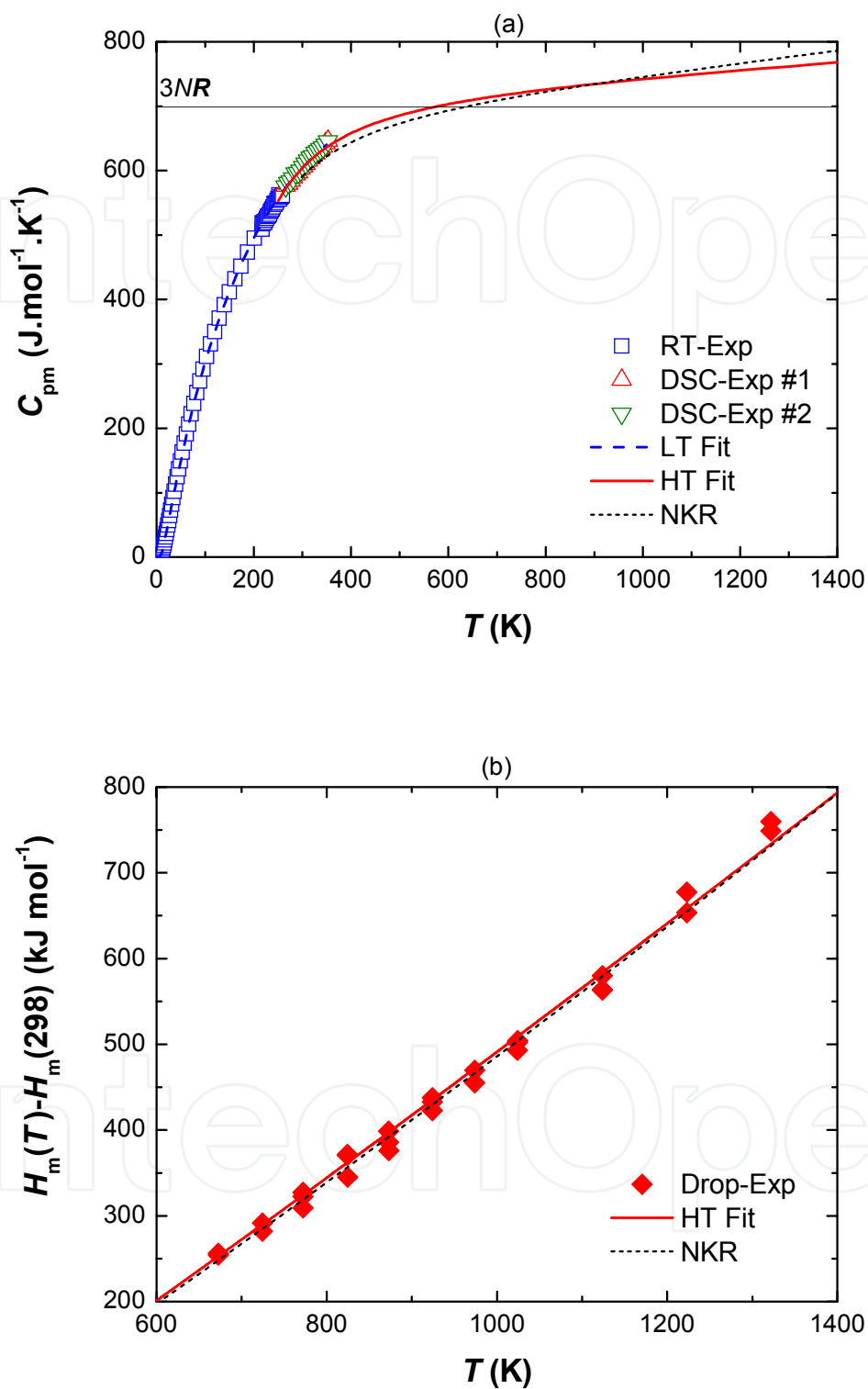


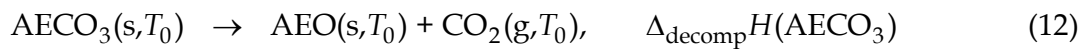
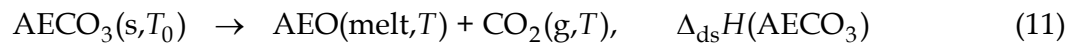
Figure 2. Temperature dependence of heat capacity (a) and relative enthalpy (b) of Bi₇Ta₃O₁₈ (3NR means the Dulong-Petit limit).

2.4. Evaluation of enthalpy of formation

The heats of drop-solution for the calcium and strontium carbonates and for the bismuth and niobium oxides were measured first. These data are necessary for the evaluation of the $\Delta_{\text{ox}}H$ values for the mixed oxides, and furthermore, these data could be compared with the literature data [49–52]. For the AECO_3 carbonates, the measured heat effect consists of three contributions:

$$\Delta_{\text{ds}}H(\text{AECO}_3, T) = \Delta_T H(\text{AECO}_3, T_0 \rightarrow T) + \Delta_{\text{decomp}}H(\text{AECO}_3, T) + \Delta_{\text{sol}}H(\text{AEO}, T) \quad (10)$$

The measurements were performed at 973 K. The values of $\Delta_{\text{ds}}H(\text{AECO}_3, 973 \text{ K})$ are given in Table 6 along with the values of $\Delta_{\text{ds}}H(\text{AEO}, 973 \text{ K})$, which were derived based on the following thermochemical cycle ($T_0 \approx 298 \text{ K}$):



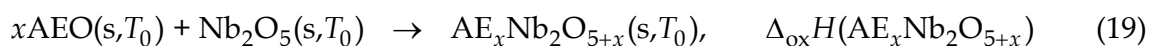
$$\Delta_{\text{ds}}H(\text{AEO}) = \Delta_{\text{ds}}H(\text{AECO}_3) - \Delta_{\text{decomp}}H(\text{AECO}_3) - \Delta_T H(\text{CO}_2) \quad (15)$$

The values $\Delta_{\text{decomp}}H(\text{CaCO}_3, 298 \text{ K}) = 178.8 \text{ kJ mol}^{-1}$, $\Delta_{\text{decomp}}H(\text{SrCO}_3, 298 \text{ K}) = 233.9 \text{ kJ mol}^{-1}$ and $\Delta_T H(\text{CO}_2, 298 \rightarrow 973 \text{ K}) = 32.0 \text{ kJ mol}^{-1}$ [53] were used for the calculations.

Next, the $\Delta_{\text{ds}}H$ values of the binary oxides Bi_2O_3 and Nb_2O_5 were measured. Because the dissolution of Nb_2O_5 and of the mixed oxides at 973 K proceeds rather slowly, the higher temperature of 1073 K was used. The measured values $\Delta_{\text{ds}}H$ are also given in Table 6.

The experimental values of $\Delta_{\text{ds}}H$ for SrCO_3 and CaCO_3 are in quite good agreement with the literature data [49–51]. On the other hand, our results and the published [52] values of $\Delta_{\text{ds}}H(\text{Nb}_2\text{O}_5)$ are quite different. It should be noted that a more endothermic value $\Delta_{\text{decomp}}H(\text{SrCO}_3, 298 \text{ K}) = 249.4 \text{ kJ mol}^{-1}$ is presented in the literature [45], which results in more exothermic value for $\Delta_{\text{ds}}H(\text{SrO})$ by 15.5 kJ mol^{-1} .

$\Delta_{\text{ds}}H$ for the mixed oxides was measured at 1073 K. The following thermochemical cycle was used for the calculation of $\Delta_{\text{ox}}H$ for calcium and strontium niobates ($T_0 \approx 298 \text{ K}$):



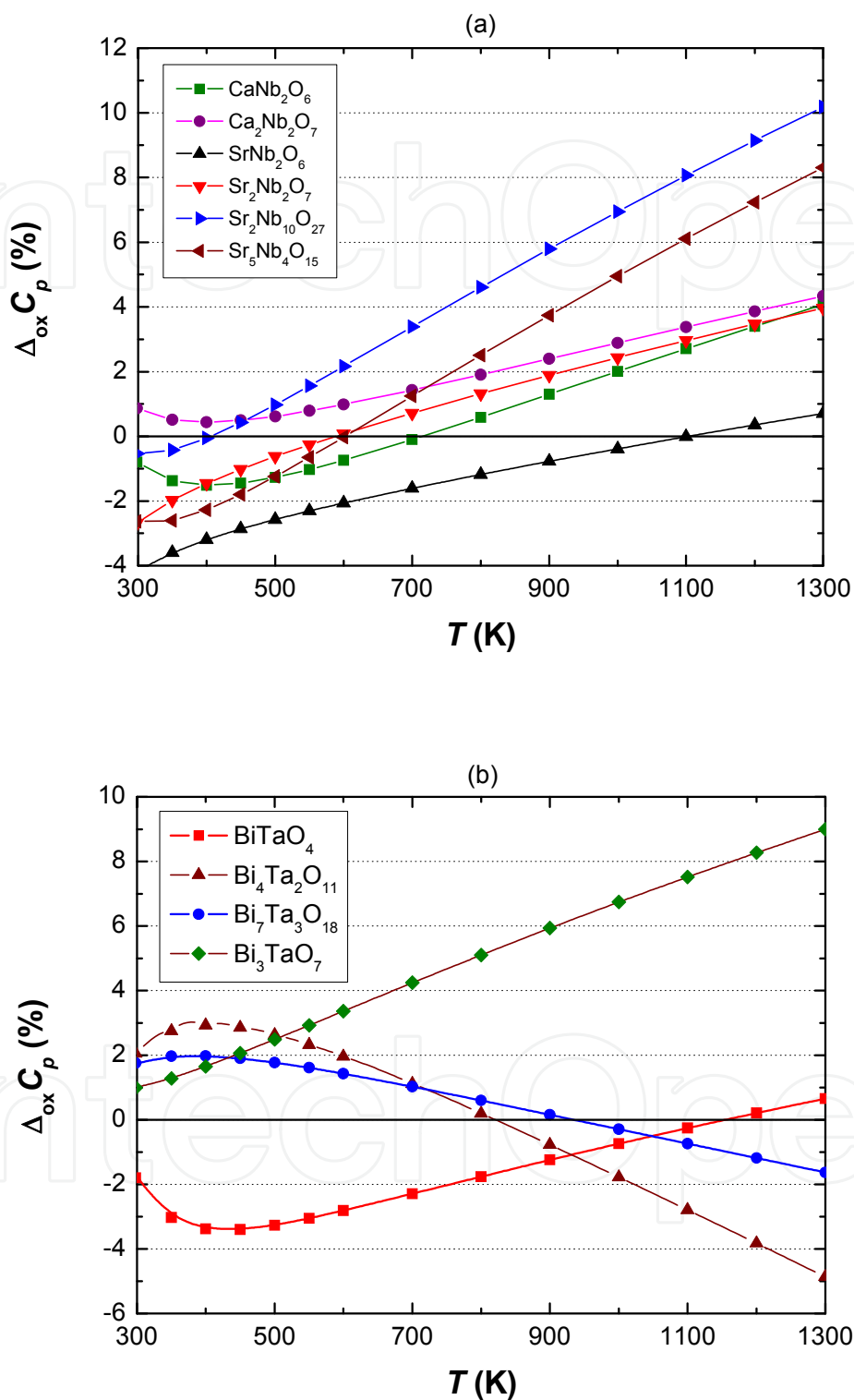


Figure 3. Temperature dependences of $\Delta_{\text{ox}} C_{p,m}$ for various mixed oxides in the systems CaO–Nb₂O₅, and SrO–Nb₂O₅ (a) and Bi₂O₃–Ta₂O₅ (b)

$$\Delta_{\text{ox}}H(\text{AE}_x\text{Nb}_2\text{O}_{5+x}) = x\Delta_{\text{ds}}H(\text{AEO}) + \Delta_{\text{ds}}H(\text{Nb}_2\text{O}_5) - \Delta_{\text{ds}}H(\text{AE}_x\text{Nb}_2\text{O}_{5+x}) \quad (20)$$

An analogous scheme was applied to calculate $\Delta_{\text{ox}}H(\text{BiNbO}_4)$. All of the experimental and calculated values are summarized in Table 7. The $\Delta_{\text{ox}}H(298 \text{ K})$ values derived from high-temperature EMN measurements [7,8,11] for the CaO-Nb₂O₅ oxides and the assessed values from the phase diagram for the SrO-Nb₂O₅ oxides [12] are also presented in Table 7.

Substance	T (K)	$\Delta_{\text{ds}}H$ (kJ mol ⁻¹) ^{a)}	$\Delta_{\text{ds}}H$ (kJ mol ⁻¹)
CaCO ₃	973	128.4 ± 10.1 (10)	119.70 ± 1.02 ^{b)}
CaO	973	-82.39	-90.70 ± 1.69 ^{b)}
CaO	1073	-77.04 ^{c)}	
SrCO ₃	973	131.4 ± 9.1 (7)	130.16 ± 1.66 ^{d)} 134.48 ± 1.89 ^{e)}
SrO	973	-134.47	-135.82 ± 2.48 ^{d)} -131.42 ± 1.89 ^{e)}
SrO	1073	-129.25 ^{f)}	
Bi ₂ O ₃	973	26.0 ± 2.9 (12)	
Bi ₂ O ₃	1073	39.6 ^{g)}	
Nb ₂ O ₅	1073	141.8 ± 6.0 (11)	91.97 ± 0.78 ^{h)}

^{a)} Data from the present work. The uncertainty is two standard deviations of the mean (95% confidence level), the number in parentheses is the number of experiments performed, ^{b)} From ref. [49], T = 976 K, ^{c)} The value $\Delta_{\text{T}}H(\text{CaO}, 973 \rightarrow 1073 \text{ K}) = 5.35 \text{ kJ mol}^{-1}$ [26] was used for the calculation, ^{d)} From ref. [50], T = 975 K, ^{e)} From ref. [51], T = 974 K, ^{f)} The value $\Delta_{\text{T}}H(\text{SrO}, 973 \rightarrow 1073 \text{ K}) = 5.35 \text{ kJ mol}^{-1}$ [27] was used for the calculation, ^{g)} The value $\Delta_{\text{T}}H(\text{Bi}_2\text{O}_3, 973 \rightarrow 1073 \text{ K}) = 13.61 \text{ kJ mol}^{-1}$ [28] was used for the calculation, ^{h)} From ref. [52], T = 973 K.

Table 6. Enthalpy of drop-solution in 3Na₂O + 4MoO₃ melts [30]

Substance	T (K)	$\Delta_{\text{ds}}H$ (kJ mol ⁻¹) ^{a)}	$\Delta_{\text{ox}}H(298 \text{ K})$ (kJ mol ⁻¹) ^{b)}	$\Delta_{\text{ox}}H(298 \text{ K})$ (kJ mol ⁻¹)
CaNb ₂ O ₆	1073	196.8 ± 20.7 (8)	-132.0 ± 23.8	-159.8 ^{c)} -130.1 ^{d)}
Ca ₂ Nb ₂ O ₇	1073	195.7 ± 27.8 (8)	-208.0 ± 31.9	-147.3 ^{c)} -177.5 ^{e)}
SrNb ₂ O ₆	1073	180.50 ± 15.7 (4)	-167.9 ± 19.1	-325.0 ^{f)}
Sr ₂ Nb ₂ O ₇	1073	167.54 ± 34.7 (4)	-289.2 ± 37.5	-367.4 ^{f)}
BiNbO ₄	1073	132.61 ± 8.9 (7)	-41.9 ± 11.1	

^{a)} Data from the present work. The uncertainty is two standard deviations of the mean (95% confidence level), the number in parentheses is the number of experiments performed, ^{b)} The experimental data from the present work. The uncertainty was calculated according to the error propagation law, ^{c)} From ref. [11], ^{d)} From ref. [7], ^{e)} From ref. [8], ^{f)} From ref. [12].

Table 7. Enthalpies of drop-solution in 3Na₂O + 4MoO₃ melt ($\Delta_{\text{ds}}H$) and enthalpy of formation from constituent binary oxides ($\Delta_{\text{ox}}H$) [30]

Our values for the calcium niobates are in good agreement with Raghavan's data [7,8], while the data from Dneprova et al. [11] are quite different. Moreover, a relation, $\Delta_{\text{ox}}H(\text{CaNb}_2\text{O}_6) > \Delta_{\text{ox}}H(\text{Ca}_2\text{Nb}_2\text{O}_7)$, that holds for the values from the work of Dneprova et al. is rather unexpected. The $\Delta_{\text{ox}}H$ values for strontium niobates obtained based on the binary SrO–Nb₂O₅ phase diagram evaluation [12] are substantially more exothermic than our calorimetric data. These large differences in the $\Delta_{\text{ox}}H$ values are not surprising in view of simultaneous differences in the $\Delta_{\text{ox}}S$ values from the assessment [12] and those derived from low temperature dependences of the molar heat capacity of SrNb₂O₆ and Sr₂Nb₂O₇ [24,26].

3. Empirical correlation S–V

A linear correlation between the standard molar entropy at 298.15 K and the formula unit volume $V_{\text{f.u}}$ has been proposed by Jenkins and Glaser [54–56]. This approach was used in this work for mixed oxides in the CaO–SrO–Bi₂O₃–Nb₂O₅–Ta₂O₅ system. The linear relation is obvious (see Fig. 4) and the straight line almost naturally passes through the origin:

$$S_{\text{m}}(\text{J K}^{-1}\text{mol}^{-1}) = 1680.5 V_{\text{f.u.}}(\text{nm}^3 \text{f.u.}^{-1}) \quad (21)$$

The average relative error in entropy is 8.2 %, the binary oxides CaO and Nb₂O₅ show the deviations around 20 %. It should be noted that, in this set of values, the simple analogy of NKR (Eq.(9)) provides a better prediction with an average relative error in entropy of 4.2 %.

Eq. (21) can be used for estimation of missing data. So, the estimated value $S_{\text{m}}(\text{Sr}_2\text{Ta}_2\text{O}_7) = 256.06 \text{ J K}^{-1} \text{ mol}^{-1}$ can be compared with the value $245.41 \text{ J K}^{-1} \text{ mol}^{-1}$ obtained by numeric integration of the $C_{\text{pm}}(T)/T$ dependences from zero to 298.15 K given in Ref. [1] (relative deviation of –4.3 %). Simple calculation $S_{\text{m}}(\text{Sr}_2\text{Ta}_2\text{O}_5) = 2S_{\text{m}}(\text{SrO}) + S_{\text{m}}(\text{Ta}_2\text{O}_5) = 250.25 \text{ J K}^{-1} \text{ mol}^{-1}$ gives more reliable value (relative deviation 2.0 %).

4. Empirical estimation of enthalpy of formation

There are other mixed oxides in the system CaO–SrO–Bi₂O₃–Nb₂O₅–Ta₂O₅ for which the values of enthalpy of formation $\Delta_f H$ or enthalpy of formation from binary oxides $\Delta_{\text{ox}}H$ have not yet been determined. As a rough estimate, the values of $\Delta_{\text{ox}}H$ calculated according to an empirical method proposed by the authors [56] can be used. In the case of Ca, Sr and Bi niobates the following relation holds for $\Delta_{\text{ox}}H$:

$$\frac{\Delta_{\text{ox}}H}{n_{\text{Nb}} + n_{\text{Me}}} = -2 \cdot 96.5 \alpha y x_{\text{Nb}} x_{\text{Me}}^{\delta} (X_{\text{Nb}} - X_{\text{Me}})^2 \quad (22)$$

where X_{Nb} and X_{Me} (Me = Ca, Sr or Bi) are Pauling's electronegativities of the relevant elements, x_{Nb} and x_{Me} are the molar fractions of the oxide-forming elements ($x_{\text{Nb}} = n_{\text{Nb}}/(n_{\text{Nb}} + n_{\text{Me}})$ etc.), y is the number of oxygen atoms per one atom of oxide-forming elements and α

and δ are the model parameters. Using Pauling's electronegativities, $X_{\text{Nb}} = 1.60$, $X_{\text{Ca}} = 1.00$, $X_{\text{Sr}} = 0.95$, and $X_{\text{Bi}} = 2.02$, and the calorimetric values of $\Delta_{\text{ox}}H$ obtained in this work, the values of $\alpha = 2.576$ and $\delta = 1.50$ were derived from the least-squares fit. The estimated $\Delta_{\text{ox}}H$ values for calcium and strontium niobates are shown in Fig. 5. The values of $\Delta_{\text{ox}}H$ that were calculated according to an empirical method proposed by Zhuang et al. [57] are displayed for comparison.

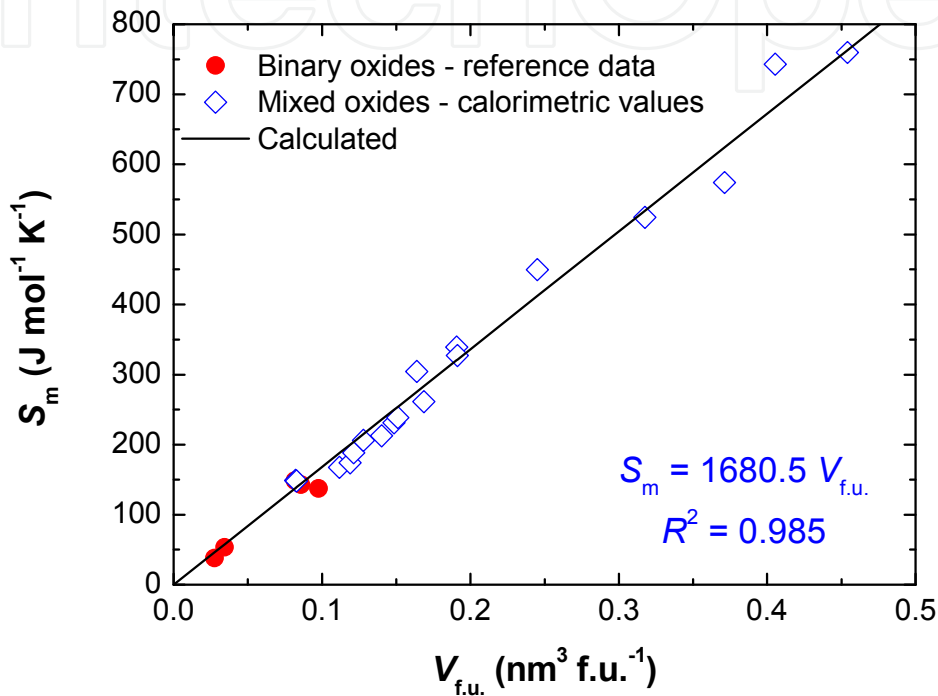


Figure 4. Correlation between the standard molar entropy at 298.15 K and the formula unit volume $V_{\text{f.u.}}$ for various mixed oxides in the system CaO–SrO– Bi₂O₃–Nb₂O₅–Ta₂O₅ (data from table Table 3)

5. Conclusion

The above presented data derived from calorimetric measurements became the basis for thermodynamic database FS-FEROX [58] compatible with the FactSage software [59,60]. Missing data for other stoichiometric mixed oxides were estimated by the empirical methods described before: the Neumann-Kopp's rule for heat capacities, the entropy-volume correlation for molar entropies and electronegativity-differences method for enthalpies of formation. At the same time, thermodynamic description of a multicomponent oxide melt was obtained analyzing relevant binary phase diagrams published in literature. The database and the FactSage software were subsequently used for various equilibrium calculations including binary T - x phase diagrams and ternary phase diagrams in subsolidus region. Thermodynamic modeling of SrBi₂Ta₂O₉ and SrBi₂Nb₂O₉ thin layers deposition from the gaseous phase were also performed to optimize the deposition conditions.

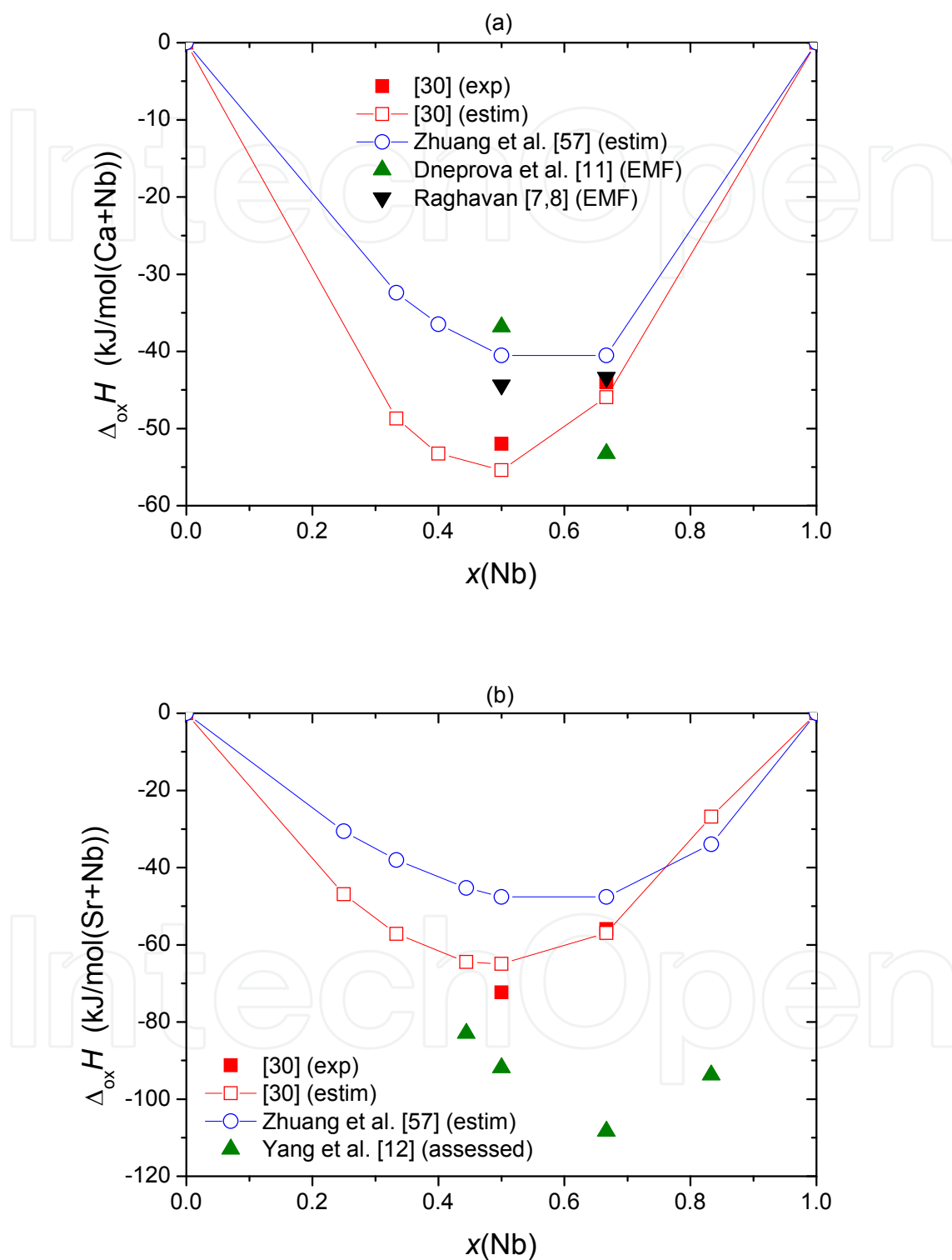


Figure 5. Values of enthalpy of formation of the mixed oxides from constituent binary oxides in the CaO–Nb₂O₅ (a) and SrO–Nb₂O₅ (b) systems (lines serve only as a guide for the eyes)

Author details

Jindřich Leitner, David Sedmidubský and Květoslav Růžička
Institute of Chemical Technology, Prague, Czech Republic

Pavel Svoboda
Charles University in Prague, Faculty of Mathematics and Physics, Prague, Czech Republic

Acknowledgment

This work was supported by the Ministry of Education of the Czech Republic (research projects N° MSM6046137302 and N° MSM6046137307). Part of this work was also supported from the Grant Agency of the Czech Republic, grant N° P108/10/1006. Low temperature experiments were performed in MLTL (<http://mltl.eu/>), which is supported within the program of Czech Research Infrastructures (project no. LM2011025).

6. References

- [1] Akishige Y, Shigematsu H, Tojo T, Kawaji H, Atake T (2005) Specific heat of $\text{Sr}_2\text{Nb}_2\text{O}_7$ and $\text{Sr}_2\text{Ta}_2\text{O}_7$. *J. Therm. Anal. Calorim.* 81: 537–540.
- [2] Shabbir G, Kojima S (2003) Acoustic and thermal properties of strontium pyroniobate single crystals. *J. Phys. D: Appl. Phys.* 36: 1036–1039.
- [3] Onodera A, Yoshio K, Myint CC, Kojima S, Yamashita H, Takama T (1999) Thermal and structural studies of phase transitions in layered perovskite $\text{SrBi}_2\text{Ta}_2\text{O}_9$. *Jpn. J. Appl. Phys.* 38: 5683–5685.
- [4] Onodera A, Yoshio K, Myint CC, Tanaka M, Hironaka K, Kojima S (2000) Thermal behavior in ferroelectric $\text{SrBi}_2\text{Ta}_2\text{O}_9$ thin films. *Ferroelectrics* 241: 159–166.
- [5] Yoshio K, Onodera A, Yamashita H (2003) Ferroelectric phase transition and new intermediate phase in bi-layered perovskite $\text{SrBi}_2\text{Ta}_2\text{O}_9$. *Ferroelectrics* 284: 65–74.
- [6] Morimoto K, Sawai S, Hisano K, Yamamoto T (1999) Simultaneous measurements of specific heat capacity and dielectric constant of ferroelectric $\text{SrBi}_2(\text{Nb}_x\text{Ta}_{1-x})_2\text{O}_9$ ceramics. *Ferroelectrics* 227: 133–140.
- [7] Raghavan S (1991) Thermodynamic stability of monocalcium niobate using calcium fluoride solid electrolyte galvanic cell. *Trans. Indian Inst. Met.* 44: 285–286.
- [8] Raghavan S (1992) Thermodynamics of formation of high calcium niobates from emf measurements. *J. Alloys Compd.* 179: L25–L27.
- [9] Raghavan S (1991) Electrochemical determination of the stability of calcium ditantalate. *Indian J. Technol.* 29: 313–314.
- [10] Raghavan S (1992) Thermodynamics of the formation of high calcium tantalates from emf measurements. *J. Alloys Compd.* 189: L39–L40.
- [11] Dneprova VG, Rezukhina TN, Gerasimov YI (1968) Thermodynamic properties of some calcium niobates. *Dokl. Akad. Nauk SSSR* 178: 135–137.

- [12] Yang Y, Yu H, Jin Z (1999) Thermodynamic calculation of the SrO–Nb₂O₅ system. *J. Mater. Sci. Technol.* 15: 203–207.
- [13] Saunders N, Miodownik AP (1998) *Calphad (Calculation of phase diagrams): A comprehensive guide*. Pergamon Materials Series, Vol. 1., Pergamon.
- [14] Hallstedt B, Risold D, Gauckler LJ (1997): Thermodynamic assessment of the bismuth–calcium–oxygen system. *J. Am. Ceram. Soc.* 80: 2629–2636.
- [15] Hallstedt B, Risold D, Gauckler LJ (1997) Thermodynamic assessment of the bismuth–strontium–oxygen system. *J. Am. Ceram. Soc.* 80: 1085–1094.
- [16] Idemoto Y, Shizuka K, Yasuda Y, Fueki K (1993) Standard enthalpies of formation of member oxides in the Bi–Sr–Ca–Cu–O system. *Physica C* 211: 36–44.
- [17] Jacob KT, Jayadevan KP (1997) Combined use of oxide and fluoride solid electrolytes for the measurement of Gibbs energy of formation of ternary oxides: System Bi–Ca–O. *Mater. Trans. JIM* 38: 427–436.
- [18] Jacob KT, Jayadevan KP (198) System Bi–Sr–O: Synergistic measurements of thermodynamic properties using oxide and fluoride solid electrolytes. *J. Mater. Res.* 13: 1905–1908.
- [19] Hallstedt B, Gauckler L (2003) Revision of the thermodynamic descriptions of the Cu–O, Ag–O, Ag–Cu–O, Bi–Sr–O, Bi–Ca–O, Bi–Cu–O, Sr–Cu–O, Ca–Cu–O and Sr–Ca–Cu–O systems *CALPHAD* 27: 177–191.
- [20] Abrman P, Sedmidubský D, Strejc A, Voňka P, Leitner J (2002) Heat capacity of mixed oxides in the Bi₂O₃–CaO system. *Thermochim. Acta* 381: 1–7.
- [21] Hampl M, Strejc A, Sedmidubský D, Růžička K, Hejtmánek J, Leitner J (2006) Heat capacity, enthalpy and entropy of bismuth niobate and bismuth tantalate. *J. Solid State Chem.* 179: 77–80.
- [22] Leitner J, Hampl M, Růžička K, Sedmidubský D, Svoboda P, Vejpravová J (2006) Heat capacity, enthalpy and entropy of strontium bismuth niobate and strontium bismuth tantalate. *Thermochim. Acta* 450: 105–109.
- [23] Hampl M, Leitner J, Růžička K, Straka M, Svoboda P (2007) Heat capacity and heat content of BiNb₅O₁₄. *J. Thermal Anal. Calorimetry* 87: 553–556.
- [24] Leitner J, Hampl M, Růžička K, Straka M, Sedmidubský D, Svoboda P. (2008) Thermodynamic properties of strontium metaniobate SrNb₂O₆. *J. Thermal. Anal. Calorimetry* 91: 985–990.
- [25] Leitner J, Hampl M, Růžička K, Straka M, Sedmidubský D, Svoboda P (2008) Heat capacity, enthalpy and entropy of strontium niobate Sr₂Nb₂O₇ and calcium niobate Ca₂Nb₂O₇. *Thermochim. Acta* 475: 33–38.
- [26] Leitner J, Růžička K, Sedmidubský D, Svoboda P (2009) Heat capacity, enthalpy and entropy of calcium niobates. *J. Thermal. Anal. Calorimetry* 95: 397–402.
- [27] Leitner J, Šipula I, Růžička K, Sedmidubský D, Svoboda P (2009) Heat capacity, enthalpy and entropy of strontium niobates Sr₂Nb₁₀O₂₇ and Sr₅Nb₄O₁₅. *J. Alloys Compd.* 481: 35–39.

- [28] Leitner J, Jakeš V, Sofer Z, Sedmidubský D, Růžička K, Svoboda P (2011) Heat capacity, enthalpy and entropy of ternary bismuth tantalum oxides. *J. Solid State Chem.* 184: 241–245.
- [29] Leitner J, Sedmidubský D, Růžička K, Svoboda P (2012) Heat capacity, enthalpy and entropy of SrBi_2O_4 and $\text{Sr}_2\text{Bi}_2\text{O}_5$. *Thermochim. Acta.* 531: 60–65.
- [30] Leitner J, Nevřiva M, Sedmidubský D, Voňka P (2011) Enthalpy of formation of selected mixed oxides in a $\text{CaO-SrO-Bi}_2\text{O}_3\text{-Nb}_2\text{O}_5$ system. *J. Alloys Compd.* 509: 4940–4943.
- [31] Lashley J.C., Hundley MF, Migliori A, Sarrao JL, Pagliuso PG, Darling TW, Jaime M, Cooley JC, Hults WL, Morales L, Thoma DJ, Smith JL, Boerio-Goates J, Woodward BF, Stewart GR, Fisher RA, Phillips NE (2003) Critical examination of heat capacity measurements made on a Quantum Design physical property measurement system. *Cryogenics* 43: 369–378.
- [32] Dachs E, Bertoldi C (2005) Precision and accuracy of the heat-pulse calorimetric technique: low-temperature heat capacities of milligram-sized synthetic mineral samples. *Eur. J. Mineral.* 17: 251–259.
- [33] Marriott RA, Stancescu M, Kennedy CA, White MA (2006) Technique for determination of accurate heat capacities of volatile, powdered, or air-sensitive samples using relaxation calorimetry. *Rev. Sci. Instrum.* 77: 096108 (3 pp).
- [34] Kennedy CA, Stancescu M, Marriott RA, White MA (2007) Recommendations for accurate heat capacity measurements using a Quantum Design physical property measurement system. *Cryogenics* 47: 107–112.
- [35] Shi Q, Snow CL, Boerio-Goates J, Woodfield BF (2010) Accurate heat capacity measurements on powdered samples using a Quantum Design physical property measurement system. *J. Chem. Thermodyn.* 42: 1107–1115.
- [36] Hwang JS, Lin KJ, Tien C (1997) Measurement of heat capacity by fitting the whole temperature response of a heat-pulse calorimeter. *Rev. Sci. Instrum.* 68: 94–101.
- [37] Schnelle W, Engelhardt J, Gmelin E (1999) Specific heat capacity of Apiezon N high vacuum grease and of Duran borosilicate glass. *Cryogenics* 39: 271–275.
- [38] Quantum Design, Physical Property Measurement System – Application Note, <http://www.qdusa.com/sitedocs/productBrochures/heatcapacity-he3.pdf> (accessed 21-12-2011).
- [39] Arblaster JW (1994) The thermodynamic properties of platinum on ITS-90, *Platinum Metals Rev.* 38: 119–125.
- [40] Rodriguez-Carvajal J (1993) Recent advances in magnetic structure determination by neutron powder diffraction. *Physica B* 192: 55–69.
- [41] Martin CA (1991) Simple treatment of anharmonic effects on the specific heat. *J. Phys.: Condens. Matter* 3: 5967–5974.
- [42] Taylor JR, Dinsdale AT (1990) Thermodynamic and phase diagram data for the CaO-SiO_2 system. *CALPHAD* 14: 71–88.

- [43] Risold D, Hallstedt B, Gauckler LJ (1996) The strontium-oxygen system. CALPHAD 20: 353–361.
- [44] Risold D, Hallstedt B, Gauckler LJ, Lukas HL, Fries SG (1995) The bismuth-oxygen system. J. Phase Equilib. 16: 223–234.
- [45] Knacke O, Kubaschewski O, Hesselmann K (1991) Thermochemical Properties of Inorganic Substances, 2nd Ed. Berlin: Springer.
- [46] Qiu L, White MA (2001) The constituent additivity method to estimate heat capacities of complex inorganic solids. J. Chem. Educ. 78: 1076–1079.
- [47] Leitner J, Chuchvalec P, Sedmidubský D, Strejc A, Abrman P (2003) Estimation of heat capacities of solid mixed oxides. Thermochim. Acta 395: 27–46.
- [48] Leitner J, Voňka P, Sedmidubský D, Svoboda P (2010) Application of Neumann-Kopp rule for the estimation of heat capacity of mixed oxides. Thermochim. Acta 497: 7–13.
- [49] Helean KB, Navrotsky A, Vance ER, Carter ML, Ebbinghaus B, Krikorian O, Lian J, Wang LM, Catalano JG (2002) Enthalpies of formation of Ce-pyrochlore, Ca_{0.93}Ce_{1.00}Ti_{2.035}O_{7.00}, U-pyrochlore, Ca_{1.46}U⁴⁺_{0.23}U⁶⁺_{0.46}Ti_{1.85}O_{7.00} and Gd-pyrochlore, Gd₂Ti₂O₇: three materials relevant to the proposed waste form for excess weapons plutonium. J. Nuclear Mater. 303: 226–239.
- [50] Cheng J, Navrotsky A (2004) Energetics of magnesium, strontium, and barium doped lanthanum gallate perovskites. J. Solid State Chem. 177: 126–133.
- [51] Xu H, Navrotsky A, Su Y, Balmer ML (2005) Perovskite Solid Solutions along the NaNbO₃-SrTiO₃ Join: Phase Transitions, Formation Enthalpies, and Implications for General Perovskite Energetics. Chem. Mater. 17: 1880–1886.
- [52] Pozdnyakova I, Navrotsky A, Shilkina L, Reznitchenko L (2002) Thermodynamic and structural properties of sodium lithium niobate solid solutions. J. Am. Ceram. Soc. 85: 379–384.
- [53] Robbie RA, Hemingway BS (1995) Thermodynamic properties of minerals and related substances at 298.15 K and 1 bar pressure and at higher temperatures, U.S. Geological Survey Bulletin, Vol. 2131, Washington.
- [54] Jenkins HDB, Glasser L (2003) Standard absolute entropy, S[°]₂₉₈, values from volume or density. 1. Inorganic materials. Inorg. Chem. 42: 8702–8708.
- [55] Jenkins HDB, Glasser L (2006) Volume-based thermodynamics: Estimations for 2:2 salts, Inorg. Chem. 45: 1754–1756.
- [56] Voňka P, Leitner J (2009) A method for the estimation of the enthalpy of formation of mixed oxides in Al₂O₃–Ln₂O₃ systems. J. Solid State Chem. 182: 744–748.
- [57] Zhuang W, Liang J, Qiao Z, Shen J, Shi Y, Rao G (1998) Estimation of the standard enthalpy of formation of double oxide. J. Alloys Compd. 267: 6–10.
- [58] Leitner J, Sedmidubský D, Voňka P. (2009) Thermodynamic database for the oxide system CaO–SrO–Bi₂O₃–Nb₂O₅–Ta₂O₅. CALPHAD XXXVIII, 17.-22.5.2009, Praha, ČR.

- [59] Bale CW, Chartrand P, Degterov SA, Eriksson G, Hack K, Ben Mahfoud R, Melançon J, Pelton AD, Petersen S (2002) FactSage thermochemical software and databases. *Calphad* 26: 189-228.
- [60] Bale CW, Bélisle E, Chartrand P, Deckerov SA, Eriksson G, Hack K, Jung IH, Kang YB, Melançon J, Pelton AD, Robelin C, Petersen S (2009) FactSage thermochemical software and databases – recent developments. *Calphad* 33: 295-311.

IntechOpen

IntechOpen